Narrow linewidth semiconductor DFB laser with linear frequency modulation for FMCW LiDAR

S. Ayotte*[a], K. Bédard[a], M. Morin[a], S. Boudreau[a], A. Desbiens[a], P. Chrétien[a], A. Babin[a], F. Costin[a], É. Girard-Deschênes[a], G. Paré-Olivier[a], L.-P. Perron[a], M. Wichmann[b], R. Korn[b], E. Baumgart[b], O. Kern[b], N. Caspers[b]

[a]TeraXion, 2716 rue Einstein, Québec, Québec, Canada G1P 4S8;

[b]Robert Bosch GmbH – Corporate Research, Robert-Bosch-Campus 1, 71272 Renningen, Germany

ABSTRACT

Monolithic distributed feedback semiconductor lasers (1550 nm) for FMCW LiDAR applications have been designed, fabricated and tested. The strong optical frequency modulation distortion observed when a standard DFB laser is modulated with a triangular current waveform is significantly mitigated in our laser. A 100 kHz frequency modulation with amplitude of 0.9 GHz and nonlinear distortion of 0.3%, calculated as the standard deviation of the optical frequency after removal of a linear fit, was measured through an unbalanced fiber interferometer. This was achieved without electronic pre-distortion of the triangular waveform. The 60 kHz intrinsic linewidth of the laser was unaffected by the modulation. Two lasers were co-packaged in a 2.6 cm^3 multi-layer ceramic package and coupled to fiber pigtails with micro-lenses. The pins of the ceramic package were soldered to a printed circuit board containing the current sources driving the lasers. This optical source was used in a two-channel LiDAR demonstrator built from off-the-shelf fiber optic components and a two-dimensional gimbal scanning mirror. This demonstrator enabled detecting a target with 10 % Lambertian reflectivity up to a distance of > 120 m and recording point clouds of different scenes. This shows that FMCW LiDAR in combination with highly coherent and linear DFB laser sources is a very promising technology for long range sensing. A version under development will include a silicon photonics chip for further integration and functionality including I/Q detection.

Keywords: FMCW LiDAR, DFB semiconductor laser, frequency modulation

1. INTRODUCTION

In addition to radar and camera sensors, the optical LiDAR is considered a necessary orthogonal sensing technology to enable autonomous driving levels 3 to 5. With their high angular resolution, LiDARs can create a detailed point cloud of the environment helping in evaluating the distance of objects or potential obstacles in the driving path for collision avoidance. A LiDAR sensor should allow detecting low and diffusely reflecting objects up to a distance between 200-300 meters in a given field-of-view, with a depth resolution of at least 30 cm and a refresh rate between 10-25 Hz. The detection should preferably be immune to the presence of extraneous light sources (e.g. sun light and other LiDARs), otherwise additional measures must be taken to reduce their influence. The sensor should be compact, robust and capable of maintaining its performance under harsh thermal and vibrational conditions usually found in vehicles. Under all circumstances, the LiDAR must be in compliance with eye safety regulations.

A first configuration considered for automotive applications is the direct time-of-flight LiDAR (dToF), in which a laser emits a periodic train of short and intense light pulses. The dToF LiDAR performs direct detection of the light reflected by a target using very sensitive and fast detectors like APDs or SPADs. The distance-to-target is determined from the time taken by light to travel to the target and back to the sensor. Direct detection complicates the rejection of extraneous light, optical filtering prior to detection being usually necessary. Unfiltered light adds to the detection noise floor and can decrease the system performance significantly. Also, no direct velocity information is available.

*sayotte@teraxion.com; phone 1 418 658-9500; fax 1 418 658-9595; teraxion.com

An optical LiDAR can also rely on a coherent detection scheme. In this case, a laser emits a highly coherent continuous stream of light. Part of the light is transmitted towards a target to be detected, whereas the rest of the light is internally directed towards the LiDAR detection unit and acts as a local oscillator (LO). Light reflected by a target to the LiDAR is mixed optically with the LO prior to photodetection. The detected optical power is thus the result of the interference between the LO and the return signal. In a frequency-modulated continuous-wave LiDAR (FMCW LiDAR), the optical frequency of the light emitted by the laser is modulated periodically in time according to a triangular function. The electrical signal resulting from photodetection then beats at an RF frequency equal to the difference between the optical frequencies of the local oscillator and of the light received by the LiDAR. The distance to target is determined from the electrical beat frequency taking into account the parameters of the frequency modulation applied to the laser light. This principle of operation is further illustrated in Fig.1, where the blue curve represents the optical frequency of the local oscillator and the red curve represents the optical frequency of the light received at the LiDAR after reflection by a target. The return signal is delayed by the time taken by the light to propagate from the LiDAR to the target and back. It is also Doppler-shifted when the target is in motion relative to the LiDAR, as shown here. In the present instance, the target is moving towards the LiDAR and the ensuing Doppler shift leads to an increase in the optical frequency of the reflected light. The green curve represents the frequency of the RF beats resulting from the interference between the local oscillator and the return signal. The RF frequency alternates between two constant values from which one can deduce the target distance and speed component towards the LiDAR[1].

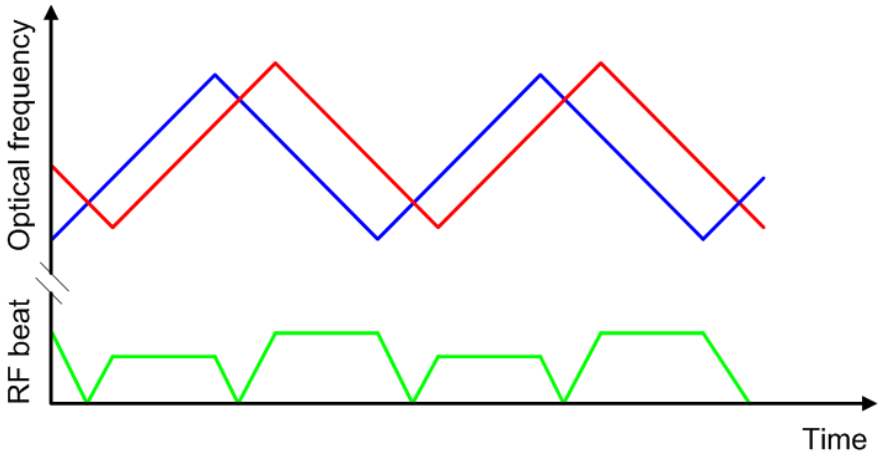

Figure 1. Optical frequency of the signal transmitted by an ideal laser in a FMCW LiDAR (blue curve), optical frequency of the signal received at the LiDAR after reflection by a moving target (red curve), RF frequency of the beats resulting from the interference between these signals (green curve)

The detection signal amplitude in a FMCW LiDAR is proportional to the square root of the product of the local oscillator optical power and the optical power of the returning light. This translates into an increased dynamic range: the FMCW LiDAR is capable of handling a larger span of returning light power than a time-of-flight LiDAR. The power of the local oscillator being typically much larger than that of the returning light, the FMCW LiDAR also produces a sizably larger electrical signal than a time-of-flight LiDAR for a given returning light optical power. The FMCW LiDAR is thus more sensitive, the local oscillator acting as an amplifier. Finally, extraneous light can be rejected more efficiently in a FMCW LiDAR because filtering is performed in the electrical domain. Most of the extraneous light from other LiDAR sensors produces electrical signals at frequencies away from the expected RF beat frequency given the laser optical frequency chirp rate (Hz/s) and the range of detection. Narrow band electrical filtering, more easily implemented than narrow band optical filtering, can dispatch most of the electrical noise caused by extraneous light very efficiently. Furthermore, the power of the local oscillator is usually set to a value ensuring that its shot noise dominates over all other noise sources. In this case, the system becomes immune to background light. Altogether, a FMCW LiDAR provides better sensitivity than a time-of-flight LiDAR and more readily addresses long-range detection of obstacles. As shown in Fig. 1, the FMCW LiDAR brings about another benefit, i.e. the capacity to measure simultaneously the distance and speed of an obstacle. This capacity stems from the Doppler effect, whereby the optical frequency of light reflected by a moving object depends on its radial speed. In a time-of-flight LiDAR, speed can only be determined as a derived quantity, i.e. as the rate of change of the target position between successive frames.

Semiconductor laser diodes are the most efficient and compact laser sources available. Furthermore, their monolithic construction makes them less susceptible to vibrations. Size, power consumption, cost and robustness wise, they are the most appropriate lasers for automotive LiDAR applications. They are driven directly by an electrical current and can be modulated at high speeds. Pulsed semiconductor lasers emitting at 905 nm are used in state-of-the-art time-of-flight LiDARs. Use of a semiconductor laser in a FMCW LiDAR is more problematic. Proper operation of this type of LiDAR relies on a laser source having at any time a narrow instantaneous linewidth: the frequency noise of the laser should be as low as possible in order to maintain a high interference contrast over range and thus, a high overall signal-to-noise ratio. Furthermore, the LiDAR operation relies on the optical frequency being modulated in a reliable and reproducible way. Ideally, the laser should provide an output with an optical frequency that varies linearly as a function of a driving signal. Semiconductor lasers provide gain over a large optical band and their short laser upper level lifetime leads to a sizable spontaneous emission. Furthermore, the index of refraction of the gain medium varies with the optical intensity. This makes the resonance properties of the laser cavity susceptible to intensity noise within the cavity. Finally, semiconductor lasers are typically short, being at most a few millimeters in length. These factors combine and translate into a sizable frequency noise. Commercial distributed feedback (DFB) semiconductor lasers typically have a linewidth of a few MHz, which translates into a coherence length that is insufficient for longer-range automotive LiDAR applications with round trip distances of 400 to 600 meters. The frequency modulation (FM) response of a semiconductor laser is also far from ideal. Modulating the current driving a semiconductor laser leads to a modulation of the temperature and of the carrier density inside the laser. Both mechanisms contribute to the modulation of the index of refraction and thus to the modulation of the optical frequency emitted by the laser. The carrier density modulation is characterized by a wideband frequency response that is flat up to many GHz. Such is not the case for the temperature modulation with a bandwidth of a few hundreds of kHz. In a FMCW LiDAR modulated for example at 100 kHz, the temperature modulation taking place inside the semiconductor laser leads to a sizable distortion of the output optical frequency modulation. A triangular frequency modulation can then be achieved only with a precompensation of the driving current modulation that depends on the laser being used and the quality of heat sinking.

This paper presents a highly linear, narrow linewidth semiconductor laser suitable for automotive FMCW LiDAR applications without the need for precompensation of the drive current modulation. Section 2 discusses the characterization of the laser whereas Section 3 presents some first LiDAR results. Section 4 highlights future work involving the use of silicon photonics (SiP) chips to incorporate receiving LiDAR components and transform a LiDAR transmitter into a LiDAR transceiver.

2. LASER CHARACTERIZATION

2.1 Description

The laser was developed in collaboration with the National Research Council Canada. It consists in a monolithic distributed feedback semiconductor laser. The InGaAsP multiple quantum well (MQW) gain medium is designed for emission at the wavelength of 1550 nm. The distributed grating retroaction and coated facets ensure the oscillation of a single longitudinal mode and a narrow linewidth. Furthermore, the laser source design drastically reduces the thermal contribution to the frequency modulation. As a result, the strong optical frequency modulation distortion observed when a standard DFB laser is modulated with a triangular current waveform is significantly mitigated. Two lasers were co-packaged in a 2.6 cm^3 multi-layer ceramic package and coupled to fiber pigtails with micro-lenses. The pins of the ceramic package were soldered to a printed circuit board containing the low noise current sources driving the lasers. Figure 2 presents the optical engine including the lasers and their coupling micro-optics as well as an external view of the complete laser module.

2.2 Static performance

Table 1 presents the main characteristics of the outputs from a twin laser module. The optical power measured at the distal end of each fiber pigtails exceeds 25 mW. Both lasers emit at close to 1547.7 nm. The power spectral density of the frequency noise (PSDFN) was measured using an interferometer in quadrature as a frequency discriminator[2]. The frequency noise values given in the table were read at 10 MHz and are representative of the white frequency noise observed at high frequencies. The Lorentzian linewidths associated to the high frequency noise and calculated as $\pi \times$PSDFN are below 60 kHz. The relative intensity noise (RIN) of both lasers was measured to be -160.7 dBc/Hz at a frequency of 1 MHz.

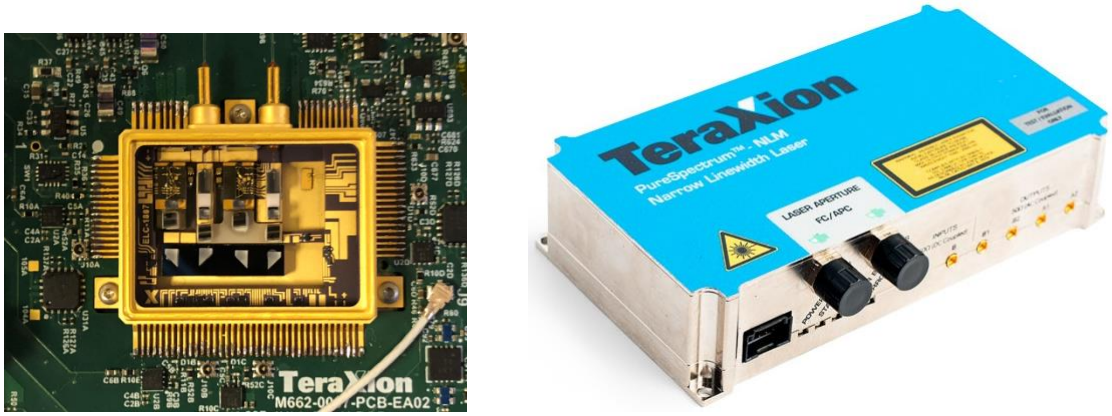

(a) (b)

Figure 2. (a) Optical engine including two lasers and their micro-optics for coupling into fiber pigtails; (b) external view of the laser source

Table 1. Characteristics of the laser module outputs

	Laser A	**Laser B**
Optical power	29 mW	25 mW
Wavelength	1547.735 nm	1547.752 nm
Frequency noise @ 10 MHz	1.8×10^4 Hz^2/Hz	1.5×10^4 Hz^2/Hz
Linewidth	56.5 kHz	47.1 kHz
RIN @ 1 MHz	-160.7 dBc/Hz	-160.7 dBc/Hz

2.3 Frequency modulation

The frequency modulation behavior of a laser can be assessed under conditions replicating those encountered in a FMCW LiDAR with the system illustrated in Fig. 3. It comprises an all fiber Mach-Zehnder interferometer that produces the beating of two copies of the laser output delayed relatively by a time determined by the length of the fiber coil. This delay is analogous to the roundtrip time experienced by the laser reflected by a target in a FMCW LiDAR system, e.g. a 150 m fiber coil corresponds to a LiDAR-to-target distance of 108 m. Figure 4 shows the signal observed with an oscilloscope when detecting the intensity beats produced while the signal driving the laser is modulated by a triangular waveform. On the left side, a chirp in the beats is clearly visible, indicating a sizable distortion in the optical frequency of the laser under a triangular modulation. The frequency of the beats on the right hand side of the figure presents a much better uniformity.

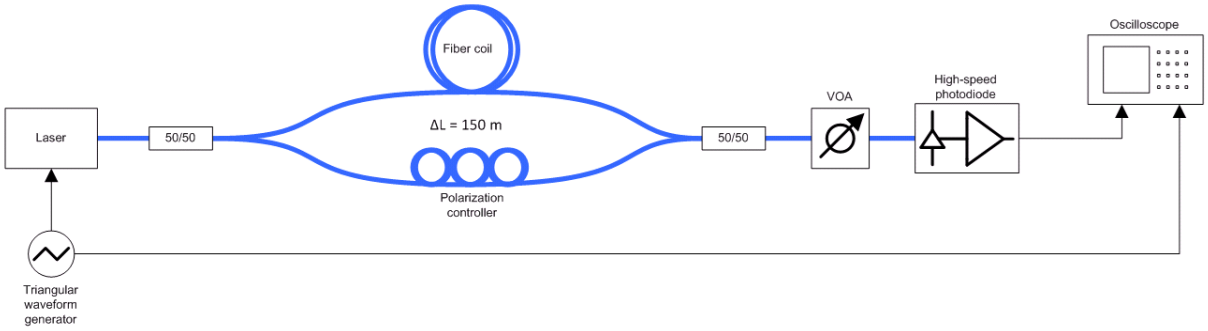

Figure 3. Characterization set-up for the measurement of the frequency distortion

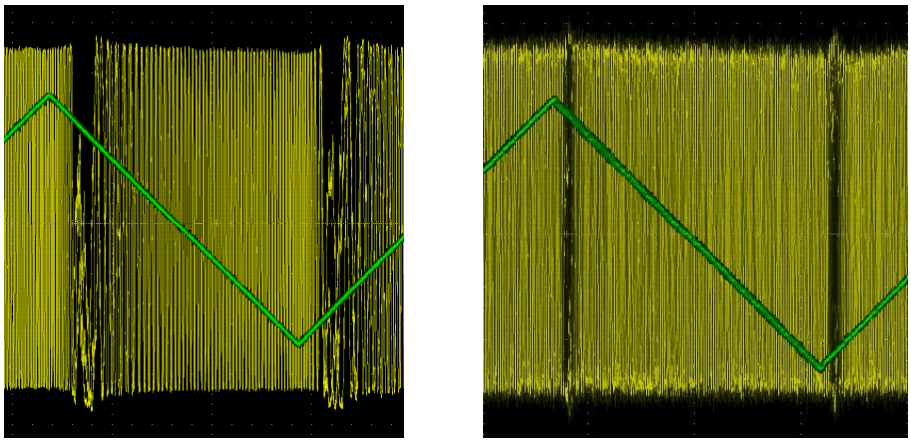

Figure 4. RF beats at the output of the characterization system as observed on an oscilloscope. A commercial DFB laser produced the beats on the left that display a visible chirp.

The time dependence of the modulated optical frequency emitted by the laser is determined from such measurements as follows. A constant amplitude optical field can be expressed as

$$E(t) \propto \exp\left[j\left(2\pi\nu_0 t + \phi(t)\right)\right] \tag{1}$$

where ν_0 is the optical carrier frequency and phase $\phi(t)$ results from fluctuations of the instantaneous optical frequency away from ν_0 due to either an applied modulation or the laser frequency noise. Such a field produces at the output of the interferometer an optical power beat signal proportional to

$$P(t) \propto \left|E(t-T/2) + E(t+T/2)\right|^2 \propto 1 + \cos\left[2\pi\nu_0 T + \phi(t+T/2) - \phi(t-T/2)\right] \tag{2}$$

where T represents the differential delay introduced by the fiber coil. The phase of the beat signal can be expressed as a function of the instantaneous optical frequency fluctuation $\delta\nu$ of the field, i.e.

$$P(t) \propto 1 + \cos\left[2\pi\nu_0 T + 2\pi\int_{t-T/2}^{t+T/2}\delta\nu(u)du\right] \tag{3}$$

The integral appearing in the cosine argument corresponds to the convolution of the frequency fluctuation with boxcar function R equal to 1 between -½ and ½ and 0 elsewhere, i.e.

$$P(t) \propto 1 + \cos\left[2\pi\nu_0 T + 2\pi\delta\nu(t) * R(t/T)\right] \tag{4}$$

The carrier frequency ν_0 cannot be unambiguously determined from a measurement of the beat signal. However, the frequency fluctuation is responsible for the time-varying phase of the beat signal, i.e.

$$\phi_{RF}(t) = 2\pi\delta\nu(t) * R(t/T) \tag{5}$$

In the frequency domain, this expression becomes

$$\tilde{\phi}_{RF}(f) = 2\pi T\delta\tilde{\nu}(f)\,\mathrm{sinc}(Tf) \tag{6}$$

The optical path difference of the interferometer thus limits the bandwidth of the optical frequency measurements. As long as the bandwidth of the optical frequency content is much smaller than $1/T$, expression (6) can be approximated by

$$\tilde{\phi}_{RF}(f) \approx 2\pi T \delta\tilde{\nu}(f) \tag{7}$$

so that

$$\delta\nu(t) \approx \frac{\phi_{RF}(t)}{2\pi T} \tag{8}$$

The phase of the interferogram corresponding to a single frequency sweep is first extracted from the associated analytical signal[3]. The computed phase is then converted into the optical frequency fluctuation $\delta\nu$, taking into account the optical path difference of the interferometer. A linear fit is finally subtracted from the optical frequency to obtain its nonlinear distortion on either the up-ramp or down-ramp of the triangular waveform. Figure 5 presents an example of the result of such calculations. The graph on the left presents the time variation of the optical frequency measured over a predetermined portion of a ramp of the triangular modulation. The graph on the right shows the remaining nonlinear distortion after subtraction of a linear fit. Note that thirty measurement samples are superimposed in these graphs. The thickness of the nonlinear curves results from the frequency noise of the laser. The average of the curves in the right graph is calculated and taken to represent the optical frequency distortion resulting from the laser modulation. The standard deviation of the mean curve is calculated to quantify the nonlinearity of the modulation. The average curve is finally subtracted from the thirty samples, leading to noisy flat curves. The standard deviation of these curves is taken as a measure of the laser frequency noise.

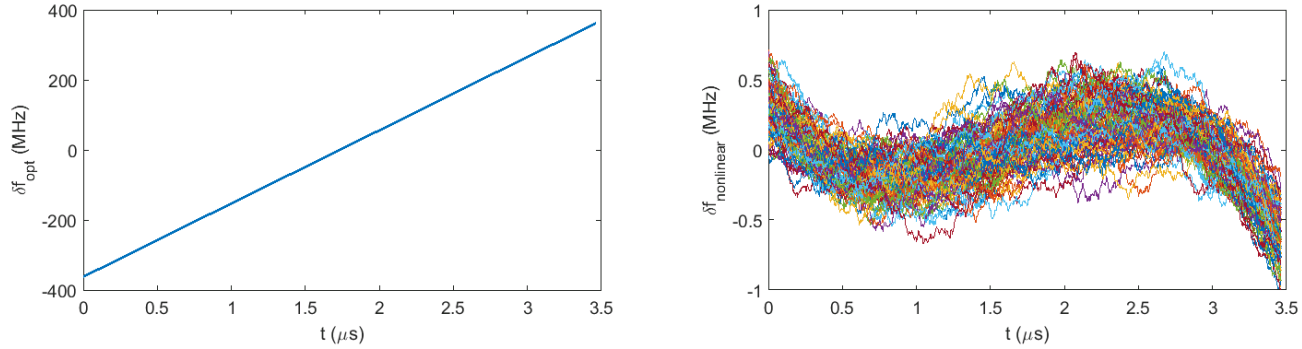

Figure 5. Optical frequency variation (left graph) and nonlinear frequency distortion after subtraction of a linear fit (right graph)

Figures 6 and 7 present the results of measurements performed when the lasers of a module were driven by a triangular modulation signal producing a 900 MHz peak-to-peak excursion of the optical frequency. Results are given for two modulation frequencies (10 kHz, 100 kHz) and fiber coil lengths varying from 10.3 to 407.6 m. At a modulation frequency of 10 kHz, the nonlinearity measurements performed over a 5 %-95 % portion of the up-ramp and down-ramp are fairly consistent as a function of the fiber coil length. The standard deviation of the nonlinearity of the lasers is seen to stand between 1.6 and 2.2 MHz, i.e. less than 0.3% of the actual optical frequency modulation. As shown previously, this represents an improvement by nearly two orders of magnitude with regards to the nonlinear distortion obtained with commercial DFB lasers[4]. At a higher modulation frequency of 100 kHz, the measured nonlinearity decreases for fiber coils longer than 50 m. This decrease results from the narrowing of the ramp portion over which the above analysis was performed from 5 %-95 % at 50.1 m to 40 %-60 % at 407.6 m, This narrowing is necessary to avoid analyzing time spans over which up-ramps and down-ramps of the relatively delayed signals coincide. Stronger filtering by the interferometers with a larger differential delay likely contributes also to the decrease in the nonlinearity observed with longer fiber coils. The nonlinearity observed at 100 kHz and with shorter fiber coils (10.3 m, 50.4 m) is comparable to that observed at 10 kHz. The measured frequency noise displays at both modulation frequencies a monotonous decrease as the fiber coil gets longer because of the ensuing reduced bandwidth of the interferometer.

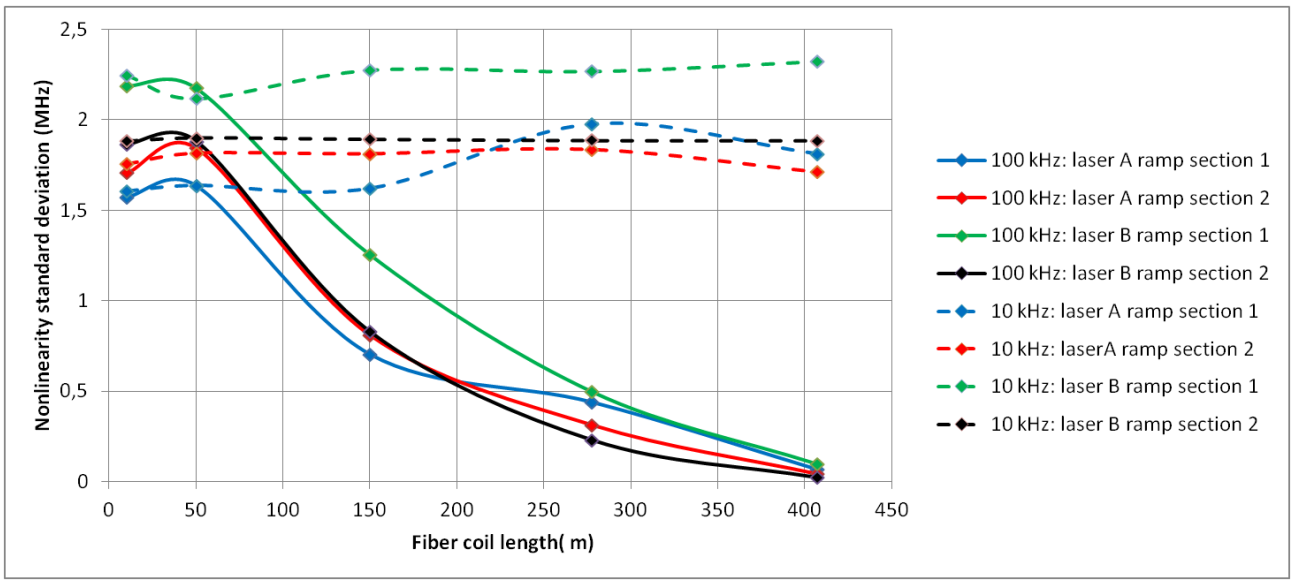

Figure 6. Nonlinearity standard deviations measured at modulation frequencies of 10 kHz and 100 kHz

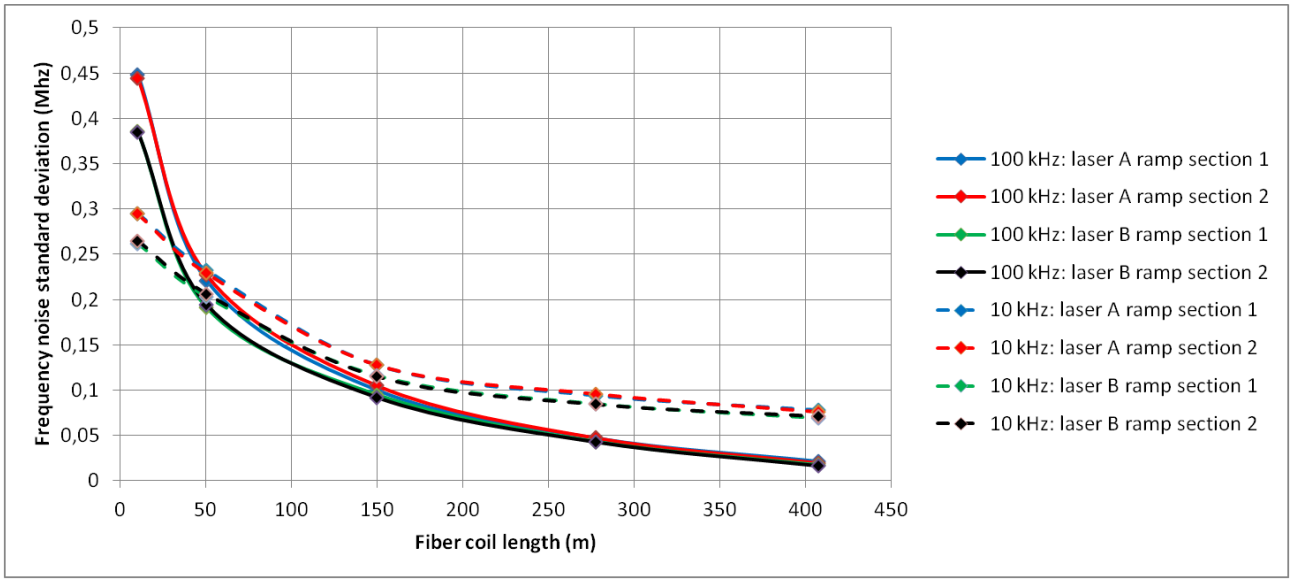

Figure 7. Frequency noise standard deviations measured at modulation frequencies of 10 kHz and 100 kHz

3. LIDAR RESULTS

The twin laser module was used in a LiDAR demonstrator built from off-the-shelf fiber optic components and a two-dimensional gimbal scanning mirror with a diameter of 15 mm. For the proof of concept, only one laser was used. The demonstrator was designed for a field-of-view of 30° x 25° with 0.1° resolution. It was operated in point-and-shoot mode at a correspondingly small frame rate (one channel only) of 0.13 Hz. Due to eye-safety regulations, the laser power was attenuated to a maximum output power of 10 mW after the outcoupling optics. In typical scanning LiDAR situations, output powers of approximately 200 mW are necessary for long range operation and typical integration times are on the order of 5 µs. The integration time was scaled by a factor of 20 in order to compensate for the penalty due to the low output

power. With a total ramp time of 100 µs, the long range performance should be comparable to that of a fast scanning unit. The laser was solely modulated with a triangular waveform generated by an external waveform generator. The overall frequency excursion was approximately 900 MHz. No additional linearization procedure or modulation pre-distortion was applied. Altogether, the demonstrator enabled the detection of a target with 10 % Lambertian reflectivity up to a distance of approx. 120 m. Furthermore, we recorded point clouds of different scenes on the Bosch research campus in Renningen, Germany, one of which is shown in Fig. 8. As can be seen, features of the buildings can be detected up to a range of approx. 180 m. Small objects like trees and lamp posts are also visible.

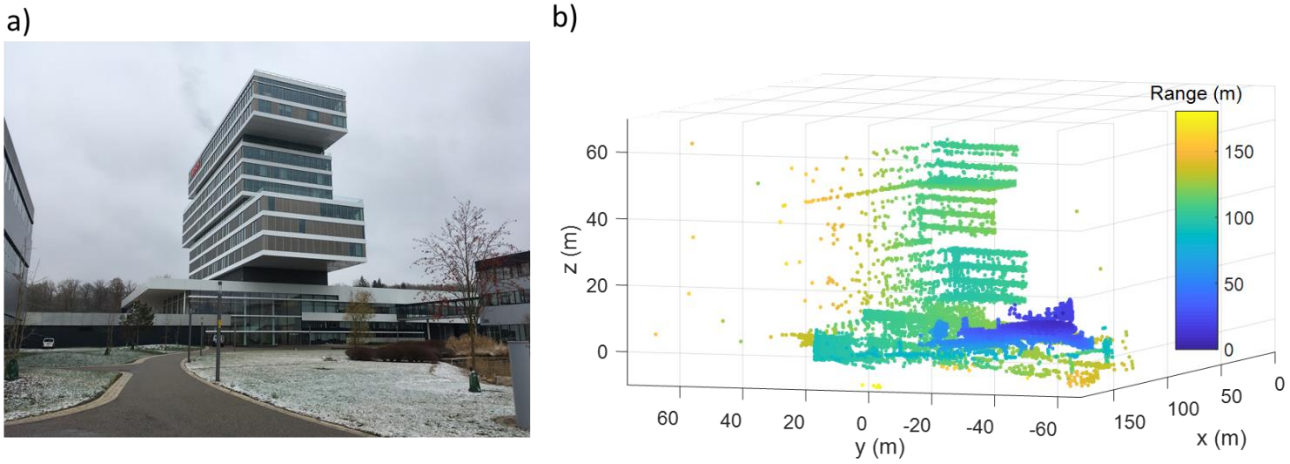

Figure 8: a) Photo of recorded LiDAR scene on Bosch campus in Renningen, b) LiDAR point cloud, range is encoded in color.

4. FUTURE WORK

The development of highly linear semiconductor lasers for FMCW LiDAR applications is still ongoing. Furthermore, work is underway to include a silicon photonics (SiP) chip in the optical engine for receiving the LiDAR return, hence improving the robustness and compactness of the LiDAR. Figure 9 illustrates a mono-axial configuration that allows bidirectional light transport in each fiber pigtail of the module. However, a 6 dB power penalty is incurred because of the 50/50 coupler at the input/output port of the LiDAR. A balanced photodetector is used to detect the beats between the LO and the return signal that are mixed with a 50/50 coupler. Figure 10 presents a biaxial configuration where each fiber pigtail transports light in a single direction. This configuration avoids the 6 dB loss found in the mono-axial configuration but requires two fiber pigtails per laser. The LO and return signal are mixed by a 2x4 optical hybrid to allow I/Q detection. Obviously, either type of mixing/detection scheme can be used in a mono-axial or biaxial configuration. Figure 11 presents the rendition of an optical engine including two SiP chips for a LiDAR having two mono-axial channels.

Concerning the laser characterization based on the LiDAR demonstrator, it is planned to use both lasers in the near future (2 channels) together with a continuously moving mirror, allowing for a higher output power. Improvements in the overall noise performance are foreseen, making shot noise limited detection possible. This in combination with the continuous scan will enable a significantly increased frame rate & range performance, also with shorter integration times.

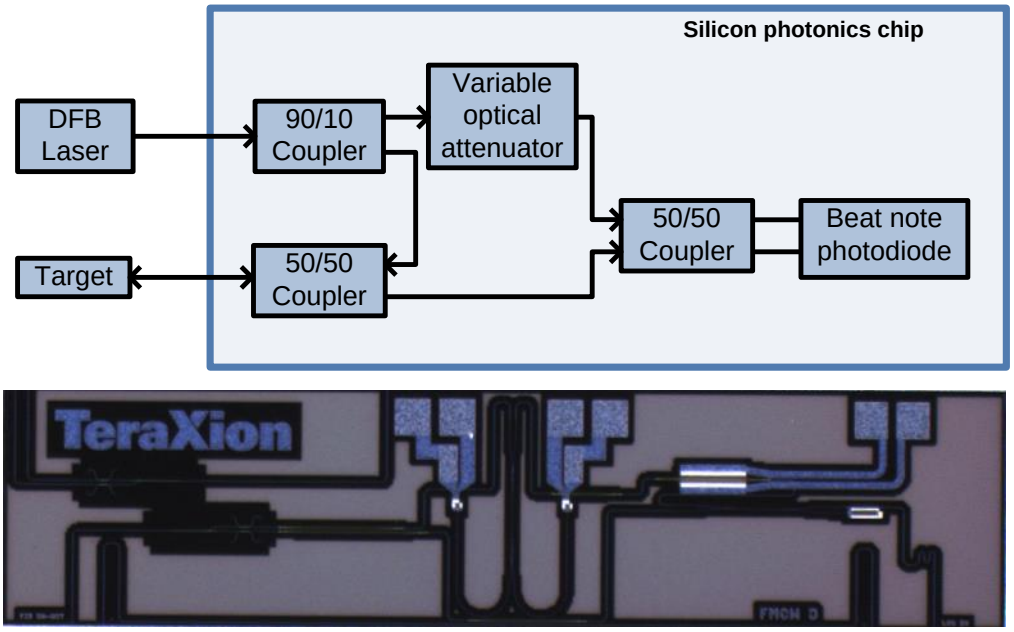

Figure 9. SiP chip for a mono-axial LiDAR transceiver.

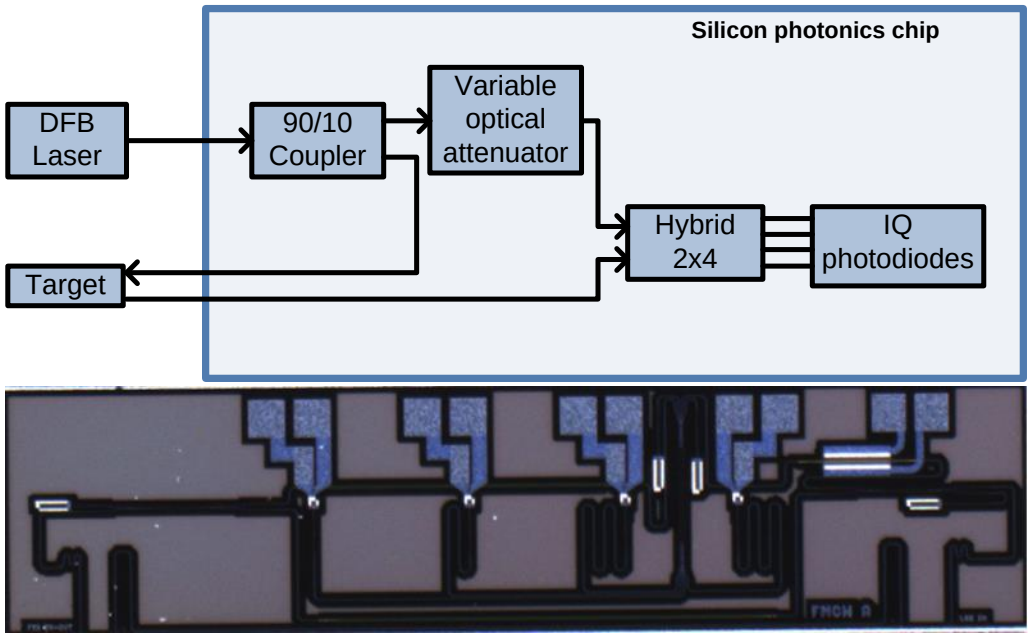

Figure 10. SiP chip for a biaxial LiDAR transceiver.

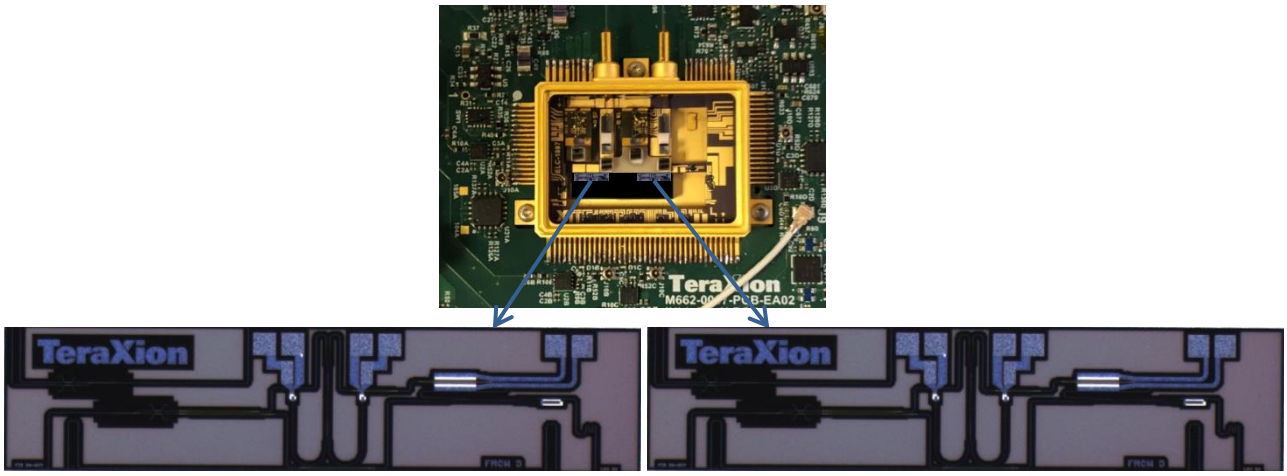

Figure 11. Rendition of an optical engine for a LiDAR with two mono-axial channels.

5. CONCLUSION

Semiconductor lasers suitable for FMCW LiDAR for autonomous vehicles have been demonstrated, making FMCW LiDAR measurements feasible without pre-compensation of the modulation signal.

ACKNOWLEDGEMENTS

TeraXion wishes to thank Drs. Greg Pakulski, Mohamed Rahim, Muhammad Mohsin, Bernard Paquette and Philip Waldron for their technical contribution to this work, as well as the team at the National Research Council Canada that supported it. TeraXion acknowledges the financial support of the National Research Council of Canada Industrial Research Assistance Program (NRC IRAP).

REFERENCES

[1] Pierrottet, D. et al., "Development of an All-Fiber Coherent Laser Radar for Precision Range and Velocity Measurements," MRS online Proceedings **883**, PROC-883-FF2.3 (2005).
[2] Cliche, J.-F., Allard, M., and Têtu, M., "High-power and ultranarrow DFB laser: the effect of linewidth reduction systems on coherence length and interferometer noise," Proc. SPIE 6216, 62160C (2006).
[3] Mandel, L. and Wolf, E., [Optical coherence and quantum optics], Cambridge University Press, New York, 92-102 (1995).
[4] Ayotte, S. et al., "Compact silicon photonics-based laser modules for FM-CW LIDAR and RFOG," Proc. SPIE 11284, 1128421 (2020).